Microdefects of Biocorroded Pipe Steel Surfaces and Safety Assessment of Localized Stress Concentrators

Pavlo Maruschak [1] [iD]**, Volodymyr Dzyura [1]** [iD]**, Olegas Prentkovskis [2],*** [iD]**, Iaroslav Lytvynenko [1] and Myroslava Polutrenko [3]**

[1] Department of Industrial Automation, Ternopil National Ivan Puuj Technical University, Ruska str. 56, 46001 Ternopil, Ukraine; maruschak.tu.edu@gmail.com (P.M.); volodymyrdzyura@gmail.com (V.D.); lytvynenko@tstu.edu.ua (I.L.)

[2] Department of Mobile Machinery and Railway Transport, Faculty of Transport Engineering, Vilnius Gediminas Technical University, Plytinės g. 27, LT-10105 Vilnius, Lithuania

[3] Ivano-Frankivsk National Technical University of Oil and Gas, Karpatska str. 15, 76019 Ivano-Frankivsk, Ukraine; polutrenkoms@gmail.com

* Correspondence: olegas.prentkovskis@vgtu.lt; Tel.: +370-5-274-4784

Abstract: The effect of sulfate-reducing bacteria (SRB) on the corrosion of steel 20 was investigated. Results demonstrated that the chemical composition of corrosion products, the corrosion rate, and corrosion type were altered due to the adherence of SRB and the subsequent formation of biofilm on the steel 20 surface. The micromechanisms of biocorrosion damage of specimens from pipe steel 20 were quantified on the basis of the microgeometry of the degraded surface and the localization parameters of corrosive stress microconcentrators. Stress concentrators in the vicinity of the micro-cuts, which are the depths of the profilograms, make it possible to evaluate safe (allowable) microcorrosion damage. The proposed approach complements the well-known methods for monitoring biodeterioration of pipe steels. With its help, it was found that a decrease in the corrosion rate of specimens with the addition of an inhibitor does not always clearly indicate its effectiveness. The case where the introduction of an inhibitor led to the destruction of the SRB biofilm on the surface of specimens from steel 20, but caused the activation of local corrosion processes and the formation of a more developed microrelief, is considered. The hollows of such microrelief are potential places of origin of defects, which require additional control.

Keywords: pipeline steel; microbiologically influenced corrosion; inhomogeneous biofilm; stress concentrators

1. Introduction

The local corrosion caused by biocorrosion factors, which accelerate the attainment of the boundary condition, causes fracture of straight sections of the main gas pipelines [1]. In addition, the pipeline life can be determined by the overall velocity and mechanisms of corrosion, which cause the dissolution of the structural elements of the material, the formation of micro- and macro-concentrators, hydrogen embrittlement, etc. [2–4]. An important task is the suppression of biocorrosion activity and the transfer of corrosion to a uniform mechanism. There are several basic methods to achieve this, including the deformation and heat treatment of pipe steels, in order to optimize the structure and provide for a more uniform distribution of alloying elements, as well as inhibiting the activity of bacteria [5,6]. The development of these approaches is the key to preventing the unpredictable origin of fatigue cracks in the pipe wall, their initiation and propagation to critical depth [7]. The technique for estimating the stress and strain localization on specimens subjected to biocorrosion is currently under development.

Most of the known approaches to estimating the microrelief of corroded surfaces are applied by parametric description of the surface profile. However, the application of these standardized criteria only allows the determination of averaged characteristics of surface micrography. Almost all of these approaches are based on the parametric description of the surface microgeometry, in which the microrelief is estimated according to the parameters R_a, R_z or R_q [8,9]. The application of such criteria is possible only under the "steady" idealized surface roughness, which is not characteristic of corrosion processes. This impairs the accuracy of the diagnostic description of the condition of the corroded surface and does not allow the determination of the degree of their damage and safety from the viewpoint of crack origin. Nonparametric methods are also known, in which such profile features as the distribution function, the density of distribution, and the asymmetry of the ordinates and tangents of the profile inclination angle are used [8,9]. However, they require further development to be suitable for the technical diagnosis of corrosion damage.

Field and laboratory studies have verified that sulfate-reducing bacteria can assist in cracking and embrittlement of pipe steels [10]. In a paper [11], a mini-review was done giving the available information on SRB-assisted cracking of pipe steels in the presence of hydrogen. The effect of hydrogen on the SRB life, as well as the combined effect of hydrogenation and biocorrosion on the strength and ductility of steels, was studied in [12]. The exhaustion of steel ductility and embrittlement of its structure makes it especially relevant to study the influence of the microrelief shape on the stress concentration in local microregions of the surface.

Taking stress concentration from biocorrosion into account is relevant not only for steels, but also for cast irons with significantly lower ductility. In particular, long-term tests (365 days) of cast iron pipes are described in [13], along with tests of external corrosion of pipes buried in soil and SRB culture medium. The pitted area of specimens with a maximum pitting depth was investigated using 3D topography, and the mechanisms of formation of distributed pits, random pits, and patch corrosion are systematized and described.

The authors of this article previously developed a new method that allows for a comparative analysis of biocorroded surfaces based on the analysis of microrelief, and the shape and depth of the surface recesses. The results were tested on several types of pipe steels and allowed not only determining the localization zones of biocorrosion, but also studying in greater detail the effectiveness of various corrosion inhibitors [14]. The problem of extending the period of nucleation and propagation of cracks is of scientific and practical importance, since its solution makes it possible to extend the life of gas pipelines, and most importantly to avoid disasters associated with sudden destruction. This can be achieved in three different ways: (a) reducing the stress intensity at the crack tip; (b) lowering stress concentration; (c) introducing residual compressive stresses [15]. In this article, an approach is developed that takes into account the influence of inhibitors not only on the decrease in the biocorrosion rate, but also in the stress concentration of biocorrosive microdefects.

The purpose of this work is to develop methods for the analysis and processing of profilometry data in order to diagnose the technical condition of surfaces damaged by biocorrosion.

2. Materials and Methods

2.1. Test Measurements

To study biocorrosion, prismatic specimens from pipe steel 20 with a size 10.0 mm × 30.0 mm × 1.0 mm cut from the pipe in the initial state were used. The chemical composition of steel 20 is given in Table 1.

Table 1. Chemical composition of steel 20.

Steel	Chemical Composition, %										
	C	Si	Mn	Ni	S	P	Cr	V	N	Cu	As
20	0.17–0.24	0.17–0.37	0.35–0.65	≤0.25	≤0.035	≤0.035	≤0.25	-	-	-	-

The specimens were cut with a water-cooled disc milling machine to avoid changes in the microstructure in the machining zone. The medium was inoculated with a cumulative sulfate-reducing bacteria (SRB) culture isolated from corrosion products in the area of local corrosion damage [16]. SRB cells of the genus *Desulfovibrio* sp. Kiev-10 were grown on Postgate B liquid medium in a thermostat at a temperature of 28 °C for 14 days. Pure sulfate-reducer colonies were obtained on Postgate B semisolid medium by means of sowing by ten-fold dilutions. In addition, the test systems inhibitors, i.e., the organic nitrogen-containing compounds, were used: inh. 1-1,8-dioxo-3,3,6,6,9-pentamethyl-10-phenyl-1,2,3,4,5,6,7,8,9,10-decahydroacridine; inh. 2-hexamethyldodecylammonium chloride. The effectiveness of the studied corrosion inhibitors was characterized by such indicators as the inhibition factor (γ) and the protective effect of the inhibitors (Z). The corrosion rate K_{gr}, (mg/(dm^2·days), was determined by gravimetric method:

$$K_{gr} = \frac{m_0 - m_f}{S \times \tau} \tag{1}$$

where m_f is the final mass of the specimen, *mg*; m_0 is the specimen mass before corrosion, *mg*; *S* is the surface area of the specimen, dm^2; τ is the exposure time, days.

The control medium was a sterile Postgate B culture medium for the cultivation of SRB bacteria. The exposure time of steel specimens was 62 days. Several schemes for the study of specimen biocorrosion were used (Table 1). The specimen roughness in the initial state and after the tests in the biocorrosion medium was estimated by the parameters of mean arithmetic deviation of the profile (R_a), the largest height of the profile irregularities (R_y), or the roughness at 10 points (R_z) of the surface topography. In order to measure surface roughness parameters a 3D Optical Surface Metrology System Leica DCM8 system was used. The surface roughness parameters were determined according to the roughness standard ISO 4288:1996 [15].

2.2. Relationship between Roughness and Stress Concentration Factor

It should be noted that in service conditions, fracture can start at the material point—the top of the microincision (in our case, the depth of the surface relief), provided that $\overline{K_t} > [K_t]$, [17,18]. Therefore, the maximum allowable stress concentration factor $[K_t]$ is a function of both the allowable depth of the profile hollow H_i and the permissible radius of its tip $[\rho]$, and the safety of the profilogram section is evaluated by calculating the radius of its profile depth. In this work, the depths of biocorrosion origin, in which bacteria, mucus, and products of their vital activity accumulated during the experiment, are considered [19,20].

The mean arithmetic deviation of the profile *Ra* was determined by averaging the absolute values of the deviations within the base length (Figure 1),

$$R_a = \frac{1}{N} \sum_{i=1}^{N} |H_i| \tag{2}$$

where *N* is the number of discrete samples of the profile; H_i is the *i*-th value of the profile.

The largest height of profile irregularities was also calculated as the distance between the projection line and the depression line within the base length [15]

$$R_y = |H_{max} - H_{min}| \tag{3}$$

where H_{max} is the height of the largest profile edge within the base length; H_{min} is the depth of the largest recess of the profile within the basic length of the profile.
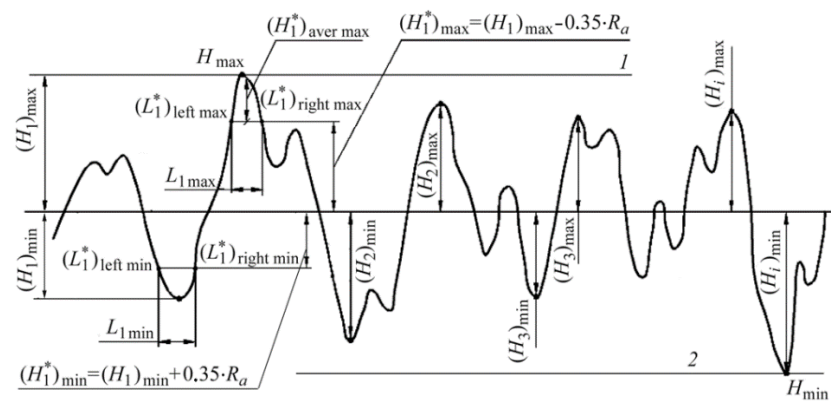
Figure 1. Profile of the surface of the samples of steel 20: 1—line of projections; 2—line of troughs.

R_z was determined as the sum of the averaged absolute height values of the five largest projections, and the depths of the five deepest depressions of the profile within the base length

$$R_z = \frac{1}{5}\left[\sum_{i=1}^{5}|(H_i)_{max}| + \sum_{i=1}^{5}|(H_i)_{min}|\right] \tag{4}$$

where $(H_i)_{max}$ are the five local maxima (vertices) of the profile; $(H_i)_{min}$ are the five local minima (depressions) of the profile.

In order to evaluate the stress concentration on the profile microgeometry, ρ_{imin}—the radii of the microrelief depressions within the analyzed profile were determined. A programmed cut of the depression profile at a distance of 0.35 R_a was performed [21]. The obtained values were averaged, and the values of the reduced radius for the 5 deepest depressions of relief were determined by the formula:

$$\overline{\rho} = \frac{1}{5}\sum_{i=1}^{5}\rho_{imin} \tag{5}$$

where ρ_{imin} are the radii for the 5 "deepest depressions" of the relief.

The morphological structure of the specimen surface is analyzed and described on the basis of evaluating the morphometric characteristics of the microirregularities. This allowed us to obtain the following results:

- based on the analysis of surface roughness and profile data, the influence of the profile depression shape on the stress localization in the vicinity of such defects was taken into account;

- to automate the microgeometry studies of the specimens, an algorithm and software were created to allow for the estimation of the microirregularities of the profile of the analyzed surfaces, in particular, the radii of the relief depressions ρ_{imin}. A decrease in the theoretical stress concentration factor causes an increase in the safe crack-like microdefect.

3. Results

It is known that the SRB corrosion of the genus *Desulfovibrio* sp. Kiev-10 occurs in pipe steels by a complex mechanism. A cathode layer of hydrogen atoms is formed on the surface. If hydrogen is not removed, it polarizes the pipe wall, causing a decrease in the corrosion rate. Using hydrogen in anaerobic respiration, SRB remove it from the surface, thereby causing depolarization and an increase in the corrosion rate (microbiologically induced) [5,6]. This results in the appearance of pitting corrosion and activation of excretion of gaseous products of microorganisms: hydrogen sulfide, phosphine, ammonia, methane, carbon dioxide, etc. and, in places, of defects in the biogenic sulfide film, and fragmentation and destruction of the pearlite phase. Ferrous sulfide was generated as an

important corrosion product due to the metabolic activity of SRB. The introduction of SRB led to the enhanced corrosion of steel 20, and the corrosion rate was closely related to the metabolic activity of SRB. In the initial state, the surface of the specimens from steel 20 had roughness R_a = 0.50 to 0.98 μm, or R_z = 3.10 to 4.09 μm. After biocorrosion exposure, there is an increase in roughness, but it is extremely heterogeneous for different test schemes (Table 2). In addition to the corrosive effect, the presence of micro-scoring and metal inflow formed by milling is crucial for the laboratory specimens to be tested. These changes in the roughness parameters are summarized in Table 3.

Table 2. Test schemes and biocorrosion rate of specimens from steel 20.

Test Schemes	Medium	K_{gr}, mg/dm^2·days
1	Postgate's medium	3.0
2	Postgate's medium + SRB	2.9
3	Postgate's medium + SRB + 1 inh. 0.5%	4.8
4	Postgate's medium + SRB + 1 inh. 1.0%	0.9
5	Postgate's medium + SRB + 2 inh. 0.5%	1.0
6	Postgate's medium + SRB + 2 inh. 1.0%	0.5

Table 3. Roughness of the initial (in the numerator) and damaged (in the denominator) surface of specimens from steel 20 under different test schemes.

Test Schemes	R_z	R_a	R_y
		μm	
1	4.09/4.12	0.50/0.67	8.24/5.16
2	4.13/7.23	0.57/0.75	6.72/9.42
3	5.30/8.95	0.98/1.53	6.65/12.03
4	4.13/5.63	0.62/0.89	5.63/6.86
5	3.61/7.66	0.52/1.24	5.15/11.04
6	3.10/22.17	0.50/2.40	3.34/39.29

Introducing inhibitors 1 and 2 in the concentration of 0.5% did not cause any stabilization of surface roughness. On the contrary, the highest increase in R_a and R_z was found for test scheme 6, i.e., 0.50 μm/2.4 μm and 3.34 μm/39.29 μm, respectively. Only with the inhibitor concentration of 1.0%, less localization of the corrosion process was observed even without a complete stabilization of the roughness. The corrosion process contributes to an increase in the surface layer roughness; for test scheme 6, the maximum increase in R_a, R_z, R_y was obtained (Table 3). This may indicate some manifestations of the biocorrosion process localization, and the formation of micropitting [22].

In the case of biocorrosion, an increase in the relief height is noticeable, which indicates the deepening of the microdefects (Figure 2). It should be noted that the parameters considered for the specimens tested under schemes 1–6 vary according to similar patterns, which indicates their identical biochemical nature. However, all of these parameters only describe the general trend of an increase in biocorrosion roughness. They can be used in areas where corrosion was relatively uniform, and no significant localization of biocorrosion was observed.
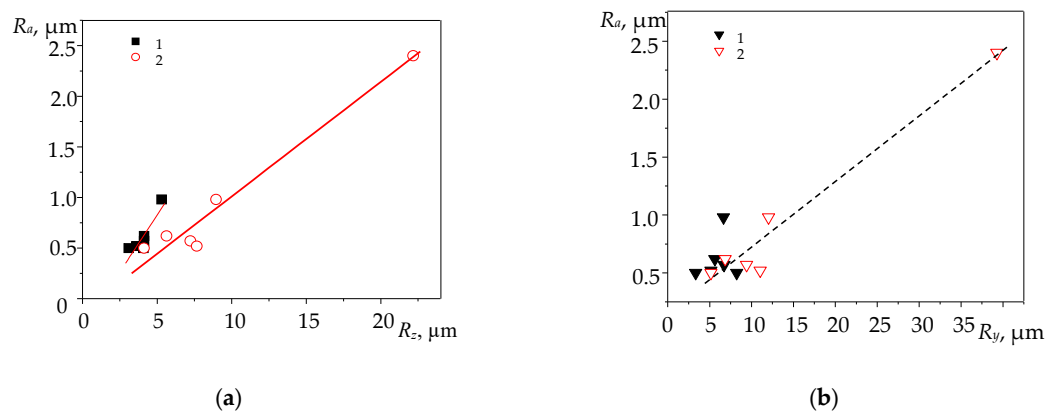
Figure 2. Dependences between roughness parameter of the initial and damaged surface of the specimens from steel 20: (**a**) $R_a – R_z$, (**b**) $R_a – R_y$; 1—initial condition; 2—after biocorrosion damage.

4. Discussion

It is noticeable that the roughness parameters only describe the surface condition in the first approximation, so the stress concentration of the corroded surfaces was estimated based on the flat section hypothesis. This approach allows establishing a connection between roughness and the quantitative parameters of fracture mechanics, which made it possible to compare the surface condition in terms of the risk of crack origin. The effective coefficient of stress concentration $\overline{K_t}$ for the corroded surfaces was determined taking into account the geometry of the profile recesses, in particular, the average radius according to the formula [15,17]:

$$\overline{K_t} = 1 + n\left(\frac{R_a}{\overline{\rho}}\right)\left(\frac{R_y}{R_z}\right) \tag{6}$$

where $\overline{\rho}$ is the mean radius of the profile recesses; n is the load type factor ($n = 2$ under static tensioning).

The effective fatigue coefficient of stress concentrations $\overline{K_f}$ associated with $\overline{K_t}$ [15,16] was calculated:

$$\overline{K_f} = 1 + q\left(\overline{K_t} - 1\right) \tag{7}$$

The sensitivity to stress concentration (q) was evaluated by the effective recess radius of the surface profile ($\overline{\rho}$) [17,18]:

$$q = \frac{1}{(1 + \gamma/\overline{\rho})} \tag{8}$$

where γ is the material constant that takes into account the conditional strength limit σ_{ys} [4].

According to the calculations, a histogram of the effective coefficient of stress concentrations $\overline{K_t}$ for different test schemes was constructed. It was found that the presence of SRB (test scheme 2, Figure 1) causes an increase of $\overline{K_t}$ from 1.23 to 2.65. According to the histogram, the following can be said: the corrosion inhibition schemes 3–5 show a decrease in the values of $\overline{K_t}$ and, accordingly, the vertices of microdefects are dissolved to larger radii. Thus, the introduction of inh. 1 at a concentration of 0.5% intensifies the corrosion processes, increases the depth, but decreases the severity of corrosion damage of the steel 20 surface to $\overline{K_t} = 1.51$. An increase in the concentration of inh. 1 to 1.0% shifts the value of $\overline{K_t}$ to 2.27. With inhibitor 2 concentration of 0.5%, $\overline{K_t} = 1.11$. In our opinion, this indicates the dispersion of bacteria along the specimen surface and a decrease in their biochemical activity and, accordingly, the bactericidal effect of the inhibitor. An increase in the concentration of inhibitor 2 to 1.0% increases the severity of the defect depth, and $\overline{K_t} = 3.23$, respectively.

In addition, $\overline{K_f}$ was calculated, but it is insensitive to the studied microrelief and ranged from 1.00 to 1.02 under the biocorrosion conditions investigated. The relative effective coefficient of stress

concentration was analyzed as the ratio of values $\lambda = \left(\overline{K_{tf}} - \overline{K_{t0}} \right) / \overline{K_{t0}}$ to the roughness parameter R_a. The histogram obtained allows the comparison of the surface condition by means of combining these two parameters. From the analysis of the data presented, it can be seen that compared to study scheme 2 (Table 1), the addition of inhibitors reduces the stress concentration in all cases except for study scheme 6. However, for schemes 4–6, this is achieved by enhancing the surface corrosion and increasing the height of microroughness. In scheme 6, the highest values of the investigated parameters are noticeable, which indicates the transition to a surface that has depressions with sharp angles.

Under force loading, the beginning of fracture processes occurs along with microfluidity in the vicinity of the microdefect. Thus, the stresses applied to the material are averaged over a significant number of microsections, as discussed above. Then, the localization of stresses in different relief depressions determines the conditions of microfluidity, and parameter $\overline{K_t}$ is useful for the comparative evaluation of the surface condition (Figure 3). In the investigated case, the initial state of the specimens was decisive when changing the microtexture of the surface. It was found earlier that an increased heterogeneity of biochemical corrosion is especially characteristic of plastically deformed areas that have structural and mechanical defects [18,23].

(**a**)　　　　　　　　　　　　　　　　　　　　　　　　　　　　　　(**b**)
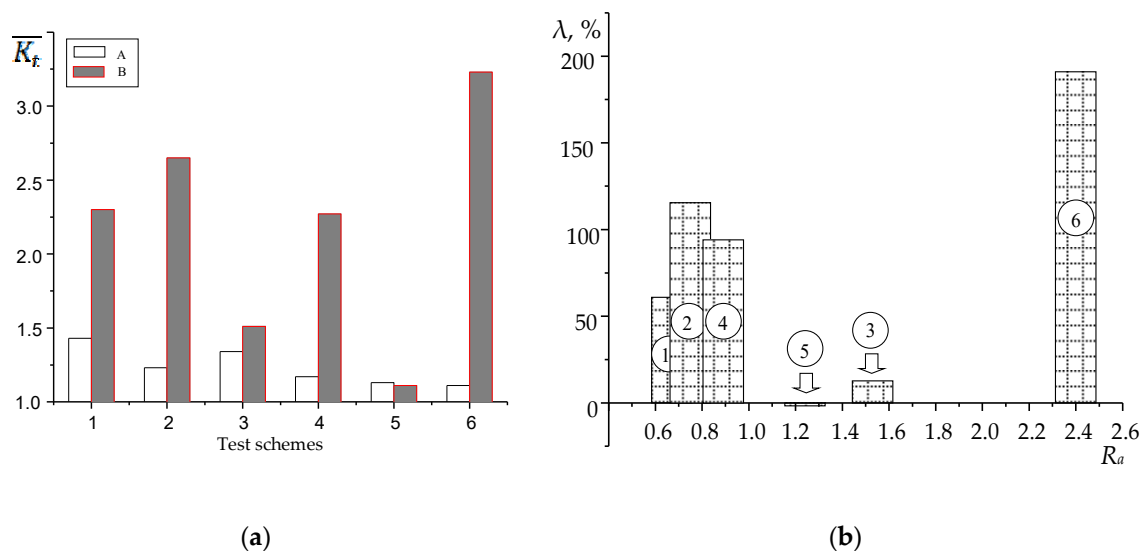
Figure 3. Stress concentration factors of the initial and damaged specimen surface from steel 20: (**a**) $\overline{K_t}$ under different test schemes, (**b**) dependence of relative effective coefficient of stress concentration (λ) from roughness parameter R_a.

It is established that the concentrators available on the investigated biocorroded surfaces are not dangerous for structural elements (Figure 3a), since $\overline{K_t} > 4$ is potentially dangerous. At a critical load of the material, such a microdefect is the point of spontaneous start of a microcrack from the top of the microrelief cavity. This is because the distribution of local stresses at the notch tip at $\overline{K_t} > 4$ is very similar to the stress-strain state of a sharp crack tip [24]. The laboratory tests conducted allow the comparison of the damage of surfaces due to biocorrosion effects. However, it is obvious that under real operating conditions, the degradation of steel 20 caused by the development of scattered damage in the main gas pipeline will reduce the resistance to biocorrosive fracture, and the action of cyclic loading may cause the exacerbation of microdefects due to the reversible plastic deformation at their tips.

The results can be successfully used to increase the information content of laboratory tests of pipe steels:

　　　- in studies of biocorrosion and efficacy of inhibitors;

　　　- when assessing the effect of inhibitors on a local defect formation and accounting for the possibility of a local microcrack start.

This will increase the stress concentration and reduce the pipe resistance to fracture within the main gas pipeline [25].

5. Conclusions

In this research, biocorrosion of a pipeline steel 20 was investigated by weight-loss testing, and surface analysis techniques. The SRB can grow well and attach to the steel surface, leading to microbiologically influenced corrosion of the steel.

Surface relief profilograms of the biocorroded specimens from steel 20 were analyzed, and the surface microgeometry was found and described using roughness parameters. The values of the effective stress concentration factors were calculated according to the Arola–Ramulu formula, taking into account the radii of the microconcentrator tips, which allowed to further substantiate the effectiveness of the proposed inhibitors. The value of $\overline{K_t}$ used in this study to assess the stress-strain state of microrelief depressions turned out to be a very sensitive parameter of surface biodeterioration; its value varied from 1.51 to 3.23.

The proposed approach provides for the normalization of the control section properties of laboratory specimens and full-scale structures by three parameters, in order to assess their tendency to generate crack-like defects, taking into account the geometric-structural properties of the surface.

It is found that a decrease in the general corrosion rate caused by adding an inhibitor does not always clearly indicate its effectiveness. The case is considered, where the introduction of an inhibitor led to the destruction of SRB films on the specimen surface and the activation of local corrosion processes. It is proved that these surface areas are potential places for defects, which require additional research.

Conflicts of Interest: The authors declare no conflict of interest.

References

1. Usher, K.M.; Kaksonen, A.H.; Cole, I.; Marney, D. Critical review: Microbially influenced corrosion of buried carbon steel pipes. *Int. Biodeterior. Biodegrad.* **2014**, *93*, 84–106. [CrossRef]
2. Polutrenko, M.S.; Maruschak, P.O.; Prentkovskis, O. The role of the biological factor in the corrosion damage of the metal of undergrund oil and gas pipelines. In Proceedings of the 20th International Conference "Transport Means", Juodkrantė, Lithuania, 5–7 October 2016; pp. 424–427.
3. Gu, T.; Jia, R.; Unsal, T.; Xu, D. Toward a better understanding of microbiologically influenced corrosion caused by sulfate reducing bacteria. *J. Mater. Sci. Technol.* **2019**, *35*, 631–636. [CrossRef]
4. Marciales, A.; Peralta, Y.; Haile, T.; Crosby, T.; Wolodko, J. Mechanistic microbiologically influenced corrosion modeling—A review. *Corros. Sci.* **2019**, *146*, 99–111. [CrossRef]
5. Jia, R.; Tan, J.L.; Jin, P.; Blackwood, D.J.; Xu, D.; Gu, T. Effects of biogenic H_2S on the microbiologically influenced corrosion of C1018 carbon steel by sulfate reducing *Desulfovibrio vulgaris* biofilm. *Corros. Sci.* **2018**, *130*, 1–11. [CrossRef]
6. AlAbbas, F.M.; Williamson, C.; Bhola, S.M.; Spear, J.R.; Olson, D.L.; Mishra, B.; Kakpovbia, A.E. Influence of sulfate reducing bacterial biofilm on corrosion behavior of low–alloy, high–strength steel (API–5L X80). *Int. Biodeterior. Biodegrad.* **2013**, *78*, 34–42. [CrossRef]
7. Zerbst, U.; Madia, M.; Klinger, C.; Bettge, D.; Murakami, Y. Defects as a root cause of fatigue failure of metallic components. III: Cavities, dents, corrosion pits, scratches. *Eng. Fail. Anal.* **2019**, *97*, 759–776. [CrossRef]
8. Gibadullin, I.N.; Valetov, V.A. Automated control of component surface microgeometry using graphic images of the profiles. *J. Instrum. Eng.* **2017**, *60*, 287–289. (In Russian) [CrossRef]

9. Gibadullin, I.N.; Valetov, V.A. Image of the surface profile as a graphic criterion of its roughness. *J. Instrum. Eng.* **2019**, *62*, 86–92. (In Russian) [CrossRef]

10. Wade, S.A.; Javed, M.A.; Palombo, E.A.; McArthur, S.L.; Stoddart, P.R. On the need for more realistic experimental conditions in laboratory-based microbiologically influenced corrosion testing. *Int. Biodeterior. Biodegrad.* **2017**, *121*, 97–106. [CrossRef]

11. Wu, T.; Sun, C.; Yan, M.; Xu, J.; Yin, F. Sulfate-reducing bacteria-assisted cracking. *Corros. Rev.* **2019**, *37*, 231–244. [CrossRef]

12. Łabanowski, J.; Rzychoń, T.; Simka, W.; Michalska, J. Sulfate-reducing bacteria-assisted hydrogen-induced stress cracking of 2205 duplex stainless steels. *Mater. Corros.* **2019**, *70*, 1667–1681. [CrossRef]

13. Wasim, M.; Djukic, M.B. Long-term external microbiologically influenced corrosion of buried cast iron pipes in the presence of sulfate-reducing bacteria (SRB). *Eng. Fail. Anal.* **2020**, *115*, 104657. [CrossRef]

14. Maruschak, P.; Konovalenko, I.; Kravets, V.; Romanyshyn, O. New methods of analysis of electron microscopic images and microprofile surfaces of biocorroded steel specimens. In Proceedings of the 7th Scientific and Technical Conference "Information Models, Systems and Technologies", Ternopil, Ukraine, 1–2 December 2019.

15. International Organization for Standardization (ISO). 4288:1996 Geometrical product specifications (GPS). In *Surface Texture: Profile Method. Rules and Procedures for the Assessment of Surface Texture*; ISO: Genève, Switzerland, 1996.

16. NACE. *TM0212-2018-SG Detection, Testing, and Evaluation of Microbiologically Influenced Corrosion on Internal Surfaces of Pipelines*; NACE International: Houston, TX, USA, 2018.

17. Arola, D.; Ramulu, M. An examination of the effects from surface texture on the strength of fiber-reinforced plastics. *J. Compos. Mater.* **1999**, *33*, 101–186. [CrossRef]

18. Arola, D.; Williams, C.L. Estimating the fatigue stress concentration factor of machined surfaces. *Int. J. Fatigue* **2002**, *24*, 923–930. [CrossRef]

19. Polutrenko, M.; Maruschak, P.; Tymoshenko, A.; Sorochak, A. Influence of soil microorganisms on metal corrosion of underground pipelines. *Koroze Ochr. Mater.* **2018**, *62*, 54–59. [CrossRef]

20. Kuang, F.; Wang, J.; Yan, L.; Zhang, D. Effects of sulfate–reducing bacteria on the corrosion behavior of carbon steel. *Electrochim. Acta* **2007**, *52*, 6084–6088. [CrossRef]

21. Kragelsky, I.V.; Rudzit, Y.A. Method of determining the mean values of the radii of curvature of the asperity tips of a roughness profile. *Proborostroyenie* **1968**, *3*, 15–24.

22. Pogrebova, I.S.; Kozlova, I.A.; Purish, L.M.; Gerasika, S.E.; Tuovinen, O.H. Mechanism of inhibition of corrosion of steel in the presence of sulfate-reducing bacteria. *Mater. Sci.* **2001**, *37*, 754–761. [CrossRef]

23. Polutrenko, M.; Maruschak, P.; Prentkovskis, O.; Tymoshenko, A.; Maruschak, O. Impact of Sulfate Reducing Bacteria on Biocorrosion of Pipeline Steels. In *Reliability and Statistics in Transportation and Communication—2018, Lecture Notes in Networks and Systems*; Kabashkin, I., Yatskiv, I., Prentkovskis, O., Eds.; Springer: Berlin/Heidelberg, Germany, 2019; Volume 68, pp. 530–538. [CrossRef]

24. Khamaza, L.A. Generalized diagram of the ultimate nominal stresses (endurance limit) and the corresponding dimensions of the non-propagating fatigue cracks for sharp and blunt notches. *Strength Mater.* **2019**, *51*, 350–360. [CrossRef]

25. Maruschak, P.; Panin, S.; Vlasov, I.; Prentkovskis, O.; Danyliuk, I. Structural levels of the nucleation and growth of fatigue crack in 17Mn1Si steel pipeline after long-term service. *Transport* **2015**, *30*, 15–23. [CrossRef]